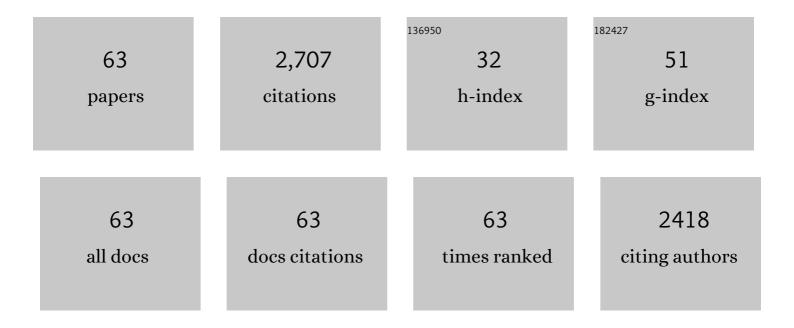
Jinquan Wan

List of Publications by Year in descending order

Source: https://exaly.com/author-pdf/1210427/publications.pdf Version: 2024-02-01



Ιινομαν Μαν

| # | Article | IF | CITATIONS |
|----|---|------|-----------|
| 1 | Fiber characterization of old corrugated container bleached pulp with laccase and glycine pretreatment. Biomass Conversion and Biorefinery, 2023, 13, 583-592. | 4.6 | 6 |
| 2 | Fe-N-C catalyst with Fe-NX sites anchored nano carboncubes derived from Fe-Zn-MOFs activate peroxymonosulfate for high-effective degradation of ciprofloxacin: Thermal activation and catalytic mechanism. Journal of Hazardous Materials, 2022, 424, 127380. | 12.4 | 91 |
| 3 | Targeted degradation of TBBPA using novel molecularly imprinted polymer encapsulated C-Fe-Nx nanocomposite driven from MOFs. Journal of Hazardous Materials, 2022, 424, 127499. | 12.4 | 24 |
| 4 | Efficient Shaping of Cellulose Nanocrystals Based on Allomorphic Modification: Understanding the Correlation between Morphology and Allomorphs. Biomacromolecules, 2022, 23, 687-698. | 5.4 | 1 |
| 5 | Modulated construction of Fe-based MOF via formic acid modulator for enhanced degradation of sulfamethoxazole:Design, degradation pathways, and mechanism. Journal of Hazardous Materials, 2022, 429, 128299. | 12.4 | 74 |
| 6 | A novel polydopamine-modified metal organic frameworks catalyst with enhanced catalytic performance for efficient degradation of sulfamethoxazole in wastewater. Chemosphere, 2022, 297, 134100. | 8.2 | 20 |
| 7 | Targeted degradation of dimethyl phthalate by activating persulfate using molecularly imprinted Fe-MOF-74. Chemosphere, 2021, 270, 128620. | 8.2 | 37 |
| 8 | Electrocatalytic oxidation of ciprofloxacin by Co-Ce-Zr/Î ³ -Al2O3 three-dimensional particle electrode. Environmental Science and Pollution Research, 2021, 28, 43815-43830. | 5.3 | 10 |
| 9 | Enhanced electro-Fenton catalytic performance with in-situ grown Ce/Fe@NPC-GF as self-standing cathode: Fabrication, influence factors and mechanism. Chemosphere, 2021, 273, 130269. | 8.2 | 50 |
| 10 | In situ synthesis of FeOCl@MoS2 on graphite felt as novel electro-Fenton cathode for efficient degradation of antibiotic ciprofloxacin at mild pH. Chemosphere, 2021, 273, 129747. | 8.2 | 32 |
| 11 | Water stable SiO2-coated Fe-MOF-74 for aqueous dimethyl phthalate degradation in PS activated medium. Journal of Hazardous Materials, 2021, 411, 125194. | 12.4 | 46 |
| 12 | Insight into degradation mechanism of sulfamethoxazole by metal-organic framework derived novel magnetic Fe@C composite activated persulfate. Journal of Hazardous Materials, 2021, 414, 125598. | 12.4 | 67 |
| 13 | Modeling the Performance of Full-Scale Anaerobic Biochemical System Treating Deinking Pulp Wastewater Based on Modified Anaerobic Digestion Model No. 1. Frontiers in Microbiology, 2021, 12, 755398. | 3.5 | 0 |
| 14 | Targeted degradation of refractory organic compounds in wastewaters based on molecular imprinting catalysts. Water Research, 2021, 203, 117541. | 11.3 | 36 |
| 15 | Fe@C activated peroxymonosulfate system for effectively degrading emerging contaminants: Analysis of the formation and activation mechanism of Fe coordinately unsaturated metal sites. Journal of Hazardous Materials, 2021, 419, 126535. | 12.4 | 33 |
| 16 | Tailored d-Band Facilitating in Fe Gradient Doping CuO Boosts Peroxymonosulfate Activation for High Efficiency Generation and Release of Singlet Oxygen. ACS Applied Materials & Interfaces, 2021, 13, 49982-49992. | 8.0 | 32 |
| 17 | Reduced graphene oxide-supported metal organic framework as a synergistic catalyst for enhanced performance on persulfate induced degradation of trichlorophenol. Chemosphere, 2020, 240, 124849. | 8.2 | 44 |
| 18 | Selective removal and persulfate catalytic decomposition of diethyl phthalate from contaminated water on modified MIL100 through surface molecular imprinting. Chemosphere, 2020, 240, 124875. | 8.2 | 33 |

JINQUAN WAN

| # | Article | IF | CITATIONS |
|----|---|------|-----------|
| 19 | Sustainable synthesis of modulated Fe-MOFs with enhanced catalyst performance for persulfate to degrade organic pollutants. Science of the Total Environment, 2020, 701, 134806. | 8.0 | 56 |
| 20 | Facile construction of highly reactive and stable defective iron-based metal organic frameworks for efficient degradation of Tetrabromobisphenol A via persulfate activation. Environmental Pollution, 2020, 256, 113399. | 7.5 | 35 |
| 21 | Adsorption properties and mechanisms of novel biomaterials from banyan aerial roots via simple modification for ciprofloxacin removal. Science of the Total Environment, 2020, 708, 134630. | 8.0 | 59 |
| 22 | Polymer Technology for the Detection and Elimination of Emerging Pollutants. Advances in Polymer Technology, 2020, 2020, 1-2. | 1.7 | 0 |
| 23 | ZSM-5-(C@Fe) activated peroxymonosulfate for effectively degrading ciprofloxacin: In-depth analysis of degradation mode and degradation path. Journal of Hazardous Materials, 2020, 398, 123024. | 12.4 | 54 |
| 24 | A comprehensive model of N2O emissions in an anaerobic/oxygen-limited aerobic process under dynamic conditions. Bioprocess and Biosystems Engineering, 2020, 43, 1093-1104. | 3.4 | 4 |
| 25 | Removal of gentian violet and rhodamine B using banyan aerial roots after modification and mechanism studies of differential adsorption behaviors. Environmental Science and Pollution Research, 2020, 27, 9152-9166. | 5.3 | 24 |
| 26 | Occurrence and risk assessment of antibiotics in multifunctional reservoirs in Dongguan, China. Environmental Science and Pollution Research, 2020, 27, 13565-13574. | 5.3 | 13 |
| 27 | Ferrous metal-organic frameworks with strong electron-donating properties for persulfate activation to effectively degrade aqueous sulfamethoxazole. Chemical Engineering Journal, 2020, 394, 125044. | 12.7 | 83 |
| 28 | Facile preparation of iron oxide doped Fe-MOFs-MW as robust peroxydisulfate catalyst for emerging pollutants degradation. Chemosphere, 2020, 254, 126798. | 8.2 | 34 |
| 29 | Enhanced photocatalytic activity of AgNPs-in-CNTs with hydrogen peroxide under visible light irradiation. Environmental Science and Pollution Research, 2019, 26, 26389-26396. | 5.3 | 5 |
| 30 | Macroscopic and microscopic properties of fibers after enzymatic deinking of mixed office waste paper. Cellulose, 2019, 26, 9863-9875. | 4.9 | 7 |
| 31 | Ferrous metal-organic frameworks with stronger coordinatively unsaturated metal sites for persulfate activation to effectively degrade dibutyl phthalate in wastewater. Journal of Hazardous Materials, 2019, 377, 163-171. | 12.4 | 107 |
| 32 | Mathematical modelling of the internal circulation anaerobic reactor by Anaerobic Digestion Model No. 1, simultaneously combined with hydrodynamics. Scientific Reports, 2019, 9, 6249. | 3.3 | 9 |
| 33 | Catalytic hydrolysis of cellulose by phosphotungstic acid–supported functionalized metal-organic frameworks with different electronegative groups. Environmental Science and Pollution Research, 2019, 26, 15345-15353. | 5.3 | 12 |
| 34 | Investigation of factors affecting the physicochemical properties and degradation performance of nZVI@mesoSiO2 nanocomposites. Journal of Materials Science, 2019, 54, 7483-7502. | 3.7 | 14 |
| 35 | Efficient degradation of Orange G with persulfate activated by recyclable FeMoO4. Chemosphere, 2019, 214, 642-650. | 8.2 | 56 |
| 36 | Quantitative structure–activity relationship for the partition coefficient of hydrophobic compounds between silicone oil and air. Environmental Science and Pollution Research, 2018, 25, 15641-15650. | 5.3 | 2 |

Jinquan Wan

| # | Article | IF | CITATIONS |
|----|--|------|-----------|
| 37 | Synthesis of iron-based metal-organic framework MIL-53 as an efficient catalyst to activate persulfate for the degradation of Orange G in aqueous solution. Applied Catalysis A: General, 2018, 549, 82-92. | 4.3 | 131 |
| 38 | Effects of wet-pressing induced fiber hornification on hydrogen bonds of cellulose and on properties of eucalyptus paper sheets. Holzforschung, 2018, 72, 829-837. | 1.9 | 13 |
| 39 | Activation performance and mechanism of a novel heterogeneous persulfate catalyst: metal–organic framework MIL-53(Fe) with Fe ^{II} /Fe ^{III} mixed-valence coordinatively unsaturated iron center. Catalysis Science and Technology, 2017, 7, 1129-1140. | 4.1 | 132 |
| 40 | Structure and Succession of Bacterial Communities of the Granular Sludge during the Initial Stage of the Simultaneous Denitrification and Methanogenesis Process. Water, Air, and Soil Pollution, 2017, 228, 1. | 2.4 | 10 |
| 41 | Metal–Carbon Hybrid Electrocatalysts Derived from Ionâ€Exchange Resin Containing Heavy Metals for Efficient Hydrogen Evolution Reaction. Small, 2016, 12, 2768-2774. | 10.0 | 37 |
| 42 | Reaction pathway and oxidation mechanisms of dibutyl phthalate by persulfate activated with zero-valent iron. Science of the Total Environment, 2016, 562, 889-897. | 8.0 | 75 |
| 43 | Metal–organic frameworks MIL-88A with suitable synthesis conditions and optimal dosage for effective catalytic degradation of Orange G through persulfate activation. RSC Advances, 2016, 6, 112502-112511. | 3.6 | 115 |
| 44 | Degradation of refractory dibutyl phthalate by peroxymonosulfate activated with novel catalysts cobalt metal-organic frameworks: Mechanism, performance, and stability. Journal of Hazardous Materials, 2016, 318, 154-163. | 12.4 | 164 |
| 45 | Facile formation of silver nanoparticles as plasmonic photocatalysts for hydrogen production. RSC Advances, 2016, 6, 106031-106034. | 3.6 | 17 |
| 46 | Multiâ€objective optimisation for design and operation of anaerobic digestion using <scp>GAâ€ANN</scp> and <scp>NSGAâ€II</scp> . Journal of Chemical Technology and Biotechnology, 2016, 91, 226-233. | 3.2 | 47 |
| 47 | Temporal and spatial variations of contaminant removal, enzyme activities, and microbial community structure in a pilot horizontal subsurface flow constructed wetland purifying industrial runoff. Environmental Science and Pollution Research, 2016, 23, 8565-8576. | 5.3 | 30 |
| 48 | Insights into the synergy of zero-valent iron and copper oxide in persulfate oxidation of Orange G solutions. Research on Chemical Intermediates, 2016, 42, 481-497. | 2.7 | 15 |
| 49 | Application of Novel Amino-Functionalized NZVI@SiO ₂ Nanoparticles to Enhance Anaerobic Granular Sludge Removal of 2,4,6-Trichlorophenol. Bioinorganic Chemistry and Applications, 2015, 2015, 1-12. | 4.1 | 6 |
| 50 | Role of inorganic ions and dissolved natural organic matters on persulfate oxidation of acid orange 7 with zero-valent iron. RSC Advances, 2015, 5, 99935-99943. | 3.6 | 61 |
| 51 | A supramolecular structure insight for conversion property of cellulose in hot compressed water: Polymorphs and hydrogen bonds changes. Carbohydrate Polymers, 2015, 133, 94-103. | 10.2 | 15 |
| 52 | Synthesis of phosphotungstic acid-supported versatile metal–organic framework PTA@MIL-101(Fe)–NH ₂ –Cl. RSC Advances, 2015, 5, 97589-97597. | 3.6 | 11 |
| 53 | Stormwater Runoff Pollutant Loading Distributions and Their Correlation with Rainfall and Catchment Characteristics in a Rapidly Industrialized City. PLoS ONE, 2015, 10, e0118776. | 2.5 | 52 |
| 54 | Fe/S doped granular activated carbon as a highly active heterogeneous persulfate catalyst toward the degradation of Orange G and diethyl phthalate. Journal of Colloid and Interface Science, 2014, 418, 330-337. | 9.4 | 94 |

JINQUAN WAN

| # | Article | IF | CITATIONS |
|----|---|------|-----------|
| 55 | New insights into the role of zero-valent iron surface oxidation layers in persulfate oxidation of dibutyl phthalate solutions. Chemical Engineering Journal, 2014, 250, 137-147. | 12.7 | 135 |
| 56 | Fiber properties of eucalyptus kraft pulp with different carboxyl group contents. Cellulose, 2013, 20, 2839-2846. | 4.9 | 29 |
| 57 | Spatial variations in the N ₂ O emissions and denitrification potential of riparian buffer strips in a contaminated urban river. Chemistry and Ecology, 2013, 29, 529-539. | 1.6 | 7 |
| 58 | Modeling a Paper-Making Wastewater Treatment Process by Means of an Adaptive Network-Based Fuzzy Inference System and Principal Component Analysis. Industrial & Engineering Chemistry Research, 2012, 51, 6166-6174. | 3.7 | 17 |
| 59 | Modeling of a paper-making wastewater treatment process using a fuzzy neural network. Korean Journal of Chemical Engineering, 2012, 29, 636-643. | 2.7 | 7 |
| 60 | Effect of beating on recycled properties of unbleached eucalyptus cellulose fiber. Carbohydrate Polymers, 2012, 87, 730-736. | 10.2 | 80 |
| 61 | A GA-Based Neural Fuzzy System for Modeling a Paper Mill Wastewater Treatment Process. Industrial & Engineering Chemistry Research, 2011, 50, 13500-13507. | 3.7 | 9 |
| 62 | Crystal and pore structure of wheat straw cellulose fiber during recycling. Cellulose, 2010, 17, 329-338. | 4.9 | 64 |
| 63 | Effects of hemicellulose removal on cellulose fiber structure and recycling characteristics of eucalyptus pulp. Bioresource Technology, 2010, 101, 4577-4583. | 9.6 | 124 |